2301-9069 (e)
1829-8370 (p)

Kapal: Jurnal Ilmu Pengetahuan dan Teknologi Kelautan
(Kapal: Journal of Marine Science and Technology)

journal homepage : http://ejournal.undip.ac.id/index.php/kapal

Ship Maneuvering Simulation to Determine Elements of Tugboat Handling: A Case Study of Paciran Port

Esqy Dhiya'ul Fuady[1*)], I Putu Sindhu Asmara[1)], Imam Sutrisno[1)]

1) Department of Safety and Risk Engineering, Shipbuilding Institute of Polytechnic Surabaya (PPNS), Surabaya 60111, Indonesia
*) Corresponding Author: esqyfuady@gmail.com

Article Info

Keywords:
Maneuvering Modelling Group;
Ship Maneuvering;
Barge;
MATLAB Simulation

Article history:
Received: 12/06/2025
Last revised: 03/08/2025
Accepted: 04/08/2025
Available online: 11/08/2025
Published: 31/10/2025

DOI:
https://doi.org/10.14710/kapal.v22i3.74393

Abstract

Paciran Port, serving as a multipurpose facility for both cargo transport and ferry services, plays a crucial role in the transportation network of East Java province. With a significant increase in vessel visits, particularly barges carrying limestone, ensuring safety during ship berthing operations has become a critical concern. This study aims to identify the key elements of tugboat handling required for safely berthing a barge. The element consists of the percentage of tugboat capacity, the heading of the tugboat, the time series, and the duration. In this study, ship berthing maneuver simulations are based on the Maneuvering Modelling Group (MMG) method. The prediction of the ship's maneuvering motion is simulated using MATLAB software within a 3-DOF (Degree of Freedom) framework. A simulation was conducted across four scenarios by varying the environmental conditions of wind direction, wind speed, current direction, and current speed. Each environmental condition varies into two initial speeds (0 knots and 2.9 knots). The berthing speed limits follow the PIANC standard. The results show that the element of tugboat handling angle can assist the barge to safely berth under diverse environmental conditions and initial speeds, with final berthing speeds consistently below 0.3 m/s (0.58 knots), which falls within the moderate condition category according to PIANC standards. Trajectory analyses further affirmed that the barge remained within the designated Paciran Port channel throughout all simulated scenarios.

1. Introduction

Paciran Port plays a crucial role as a multipurpose port serving domestic sea transport and inter-provincial as well as inter-regency crossings, making it a vital transportation hub in East Java. There has been a significant increase in ship visits and loading/unloading activities at Paciran Port, especially involving barges carrying limestone. This increased traffic demands attention to optimizing management, services, and port infrastructure, and also raises concerns regarding the safety of ship berthing processes. Considering the ship's dynamic movement changes, the ship operator must control three segments: berthing speed, transverse distance, and closing angle, making necessary adjustments to meet the objective condition requirements. Thus, the ship will eventually be able to berth smoothly at the designated jetty [1].

Although the berthing phase has garnered significant attention from researchers, it remains one of the most formidable problems in ship maneuvering due to the associated dangers [2]. Ships are more likely to have accidents when they approach at a berthing velocity higher than what is permitted when calculating the risk range for a port [3]. Tugboat assistance is a vital component of port operations and navigational safety [4]. It is crucial to estimate the required tugboat's capacity. Inaccurate estimation can lead to a dangerous condition [5]. Therefore, this research emphasizes the need for an in-depth study regarding environmental condition limits (wind and current) and ship speed limits when entering the channel, as well as the development of standard ship berthing procedures, including tugboat capacity requirements, to ensure operational safety. The most important source of information for towing, berthing, and unberthing operations is the expertise of tugboat captains and harbor pilots. However, an efficient operation method is not available [6].

The primary benefit of the MMG model lies in its ability to accurately replicate ship maneuvering dynamics across various complex scenarios, including tugboat maneuverability [7, 8]. Wu et al. conclude that the MMG approach can be successfully used, which guarantees the accurate description of the ship's force [9]. Taimuri et. al. presented a reference method and a modular mathematical model for the motion and maneuvering trajectories of the ship. It can be concluded that the method can be used to predict the maneuvering trajectories of existing or newly built ships, as well as to indicate the evasive speed in case of contact before grounding [10]. Zhao et. al. propose a novel identification technique for 3-DOF ship maneuvering modeling to further investigate more effective identification algorithms that can solve the ship motion identification modeling challenge [11]. Engineers and scientists worldwide use MATLAB to model and solve real-world problems across various fields. Including analyzing ship maneuvering performance using the MMG Model method, where ship maneuvering movements are simulated using MATLAB. From the simulation, the results obtained are consistent with actual conditions [12]. Okuda et. al. reveal that an equivalent single rudder model is introduced for maneuvering simulations of twin-propeller and twin-rudder vessels within the context of the Maneuvering Modelling Group. The simulation results of maneuvers match with the results of free-running model tests, regarding practical application [13]. Dai et. al. investigated the maneuvering performance of the ship using an MMG model, demonstrating good agreement and revealing insights into the influence of lateral separation on turning performance and minimal impact on course stability [14]. Wicaksono et al. use the MMG model to study the maneuvering motions of a ship in calm water. It shows that the current model is appropriate for the subject ship's maneuvering motion and can be applied to other ships [15]. Iswandi et. al propose and demonstrate a new method for evaluating the performance of ship-tracking algorithms for High-Frequency Surface Wave Radar (HFSWR). The research confirmed the applicability of using the MMG model to realistically evaluate ship-tracking algorithms for HFSWR [16].

The MMG model is extensively utilised in investigations of ship maneuverability, such as the turning circle and zig-zag maneuver [17, 18], but their specific application and simulation for berthing processes at Paciran Port had not been previously explored, especially the element of tugboat handling. The simulation program uses mathematical equations for the hull, propeller, and rudder components integrated into the Maneuvering Modeling Group (MMG) method [19]. MMG simulation is capable of evaluating the ability of tugboats in assisting berthing and unberthing, and also assessing the possibility of collisions [20]. The MMG model was developed by considering environmental disturbances such as water depth, wind force and moment, and current effect [21].

This research will use a simulation method based on the Maneuvering Modelling Group (MMG) with the MATLAB program to analyze the safety of the barge berthing process at Paciran Port. This study aims to identify the key elements of tugboat handling required for safely berthing a barge. The berthing speed limitation complied with Permanent International Association of Navigation Congresses (PIANC) that provides guidance and technical advice for the sustainable design, development, and maintenance of ports, waterways, and coastal areas, such as the berthing speed recommendation for ships [22].

2. Method

Tugboat handling simulation for ship berthing refers to the Maneuvering Modeling Group (MMG). A MATLAB program is used to predict the ship's maneuvering motion in a 3-DOF (Degree of Freedom) simulation, where the X-axis represents surging motion, the Y-axis represents swaying motion, and the Z-axis represents yawing motion. Figure 1 shows the coordinate commonly used in ship dynamics to describe its motion and the variables that affect it.

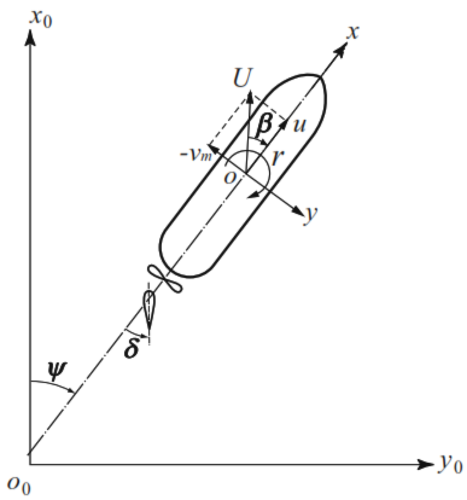

Figure 1. Coordinate System [23]

2.1. The 3 Degrees of Freedom (DOF) Equations

Equations 1 to 3 express the motion of surging, swaying, and yawing of vessels [23].

$$X = (m + m_x)\dot{u} - (m + m_y)v_m r - mx_G \quad (1)$$

$$Y = (m + m_y)\dot{v}_m - (m + m_x)ur - mx_G\dot{r} \quad (2)$$

$$N = (I_{zz} + J_{zz} + mx_G^2)\dot{r} - mx_G(\dot{v}_m + ur) \quad (3)$$

The left-hand side of Eq. 1 to Eq. 3 for X, Y, and N, are expressed as follows.

$$X = X_H + X_P + X_R + X_A + X_T \quad (4)$$

$$Y = Y_H + Y_R + Y_A + Y_T \quad (5)$$

$$N = N_H + N_R + N_A + N_T \quad (6)$$

Where the variable m denotes the vessel's mass, while mx and my represent the added mass components along the longitudinal (x) and lateral (y) axes, respectively, the ship's forward speed is represented by u (surge velocity), its sideways speed at the midpoint by vm (lateral velocity), and its rate of turn by 'r' (yaw rate). The position of the ship's center of gravity along its length is given by xG. Furthermore, IzG is the ship's moment of inertia about its center of gravity, and Jz signifies the added moment of inertia. Forces acting on the ship are described as the surge force (X), the lateral force (Y), and the yaw moment (N). Hull, propeller, rudder, wind, and tugs are denoted by the subscripts H, P, R, A, and T, respectively.

2.2. Hydrodynamic Hull Force and Moment

The hull force and moment can be expressed as follows.

$$X_H = 0{,}5\rho LdU^2(-R'_0 + X'_{vv}v'm^2 + X'_{vr}v'_m r' + X'_{vvv}r'^2 + X'_{rrr}r'^4) \quad (7)$$

$$Y_H = 0{,}5\rho LdU^2(Y'_v v'_m + Y'_r r' + Y'_{vvv}v'_m{}^3 + Y'_{vvr}v'_m{}^2 r' + Y'_{vrr}v'_m r'^2 + Y'_{rrr}r'^3) \quad (8)$$

$$N_H = 0{,}5\rho L^2 dU^2(N'_v v'_m + N'_r r' + N'_{vvv}v'_m{}^3 + N'_{vvr}v'_m{}^2 r' + N'_{vrr}v'_m r'^2 + N'_{rrr}r'^3) \quad (9)$$

L, d, and U are the Length Between Perpendiculars, the ship's draft, and the speed resultant, respectively. v'_m denotes non-dimensionalized lateral velocity defined by v_m/U and r' non-dimensionalized yaw rate by $rLpp/U$. Ship′ s maneuvering simulation requires accurate hydrodynamic derivatives [24]. Empirical formula analysis is preferred over model testing, because model testing costs a lot of time and money to simulate maneuverability at the design stage [25]. To determine the ship's resistance (R_o)Using the Holtrop Method expressed as.

$$R_o = Rf(1 + k_1) + RAPP + RW + RB + RTR + RA \quad (10)$$

Rf is frictional resistance, $(1 + k_1)$The form factor of the hull, RAPP is appendage resistance, RB is additional pressure resistance of the bulbous bow near the water surface, RTR is additional pressure resistance due to transom immersion, and RA is model-ship correlation resistance.

2.3. Hydrodynamics Derivatives

The hydrodynamic derivatives, added mass, and added moment of inertia are obtained from empirical calculations from several research [26], as shown in Table 1 - 4.

Table 1. The Formula of Added Mass and Added Moment of Inertia

Reference	Empirical Formula	
Clarke et.al. [27]	$m'_x = m' \cdot 0{,}05$	(11)
Zhou.et.al. [28]	$m'_y = m'\left[0{,}882 - 0{,}54Cb\left(1 - \frac{d}{B}\right) - 0{,}156(1 - 0{,}673Cb)\frac{L}{B} + 0{,}826\frac{d}{B}\frac{L}{B}\left(1 - 0{,}678\frac{d}{B}\right) - 0{,}638Cb\frac{d}{B}\frac{L}{B}\left(1 - 0{,}669\frac{d}{B}\right)\right]$	(12)
Yoshimura and Masumoto [29]	$J'z = m'\left[\frac{1}{100}\left(33 - 76{,}85Cb(1 - 0{,}748Cb) + 3{,}43\frac{L}{B}(1 - 0{,}63Cb)\right)\right]^2$	(13)

Table 2. The Formula of Hydrodynamic Derivatives on X-axis

Reference	Empirical Formula	
Lee et. al. [30]	$X'vv = 0{,}0014 - \left(0{,}1975d\frac{(1-Cb)}{B}\right)\frac{L}{d}$	(14)
Yoshimura and Masumoto [29]	$X'vv = 1{,}15\frac{Cb}{L/B} - 0{,}18$	(15)
Yoshimura and Masumoto [29]	$X'vvvv = -6{,}68\frac{Cb}{L/B} + 1{,}1$	(16)
Lee et. al. [30]	$X'rr = \left(-0{,}0027 + 0{,}0076Cb\frac{d}{B}\right)\frac{L}{d}$	(17)

Yoshimura and Masumoto [29]	$X'rr = -0{,}085\frac{Cb}{L/B} + 0{,}008 - x_G m'_y$	(18)

Table 3. The Formula of Hydrodynamic Derivatives on Y-axis

Reference	Empirical Formula	
Kijima et. al. [31]	$N'v = -2\frac{d}{L}$	(19)
Lee et. al. [30]	$N'v = \left(-0{,}23\frac{d}{L} + 0{,}0059\right)\frac{L}{d}$	(20)
Yoshimura and Masumoto [29]	$N'v = -2\frac{d}{L}$	(21)

Table 4. The Formula of Hydrodynamic Derivatives Acting on Yaw Moment

Reference	Empirical Formula	
Kijima et. al. [31]	$N'v = -2\frac{d}{L}$	(22)
Lee et. al. [30]	$N'v = \left(-0{,}23\frac{d}{L} + 0{,}0059\right)\frac{L}{d}$	(23)
Yoshimura and Masumoto [29]	$N'v = -2\frac{d}{L}$	(24)

2.4. Wind Force and Moment

Several factors, including wind effects, influence the ship′s maneuverability [32]. The disturbance force and moment of wind on ships maneuvering can be calculated as follows.

$$X_A = \frac{1}{2}\rho_a V_A^2 A_T C_{XA}(\theta_A) \tag{25}$$

$$Y_A = \frac{1}{2}\rho_a V_A^2 A_L C_{YA}(\theta_A) f_A(\emptyset) \tag{26}$$

$$N_A = \frac{1}{2}\rho_a V_A^2 L A_L C_{NA}(\theta_A) f_A(\emptyset) \tag{27}$$

where ρ_a is air density, A_T is the transverse projected area, A_L is the lateral projected area. $C_{XA}, C_{YA}, and\ C_{NA}$ are aerodynamic force coefficients concerning surge force, lateral force, and yaw moment, respectively. θ_A is relative wind direction, f_A is the correction coefficient when the ship heels, and $\emptyset$ is roll angle. Va is the relative wind velocity calculated as follows.

$$V_A^2 = u_A^2 + vV_A^2 \tag{28}$$

$$u_A = u + U_W \cos(\theta_W - \psi) \tag{29}$$

$$v_A = v + U_W \sin(\theta_W - \psi) \tag{30}$$

Where U_W is absolute wind velocity, θ_W is the absolute wind direction, and ψ is ships heading [33][34].

2.5. Tug Force and Moment

Tug forces and moment can be calculated by using Eq. 31-33, where F_T denotes the tug's force, Θ_T is the relative direction of the tug force, and L/2 denotes the arm of the tug moment [35].

$$XT = F_T cos\theta_T \tag{31}$$

$$YT = F_T sin\theta_T \tag{32}$$

$$NT = Y_T(L/2) \tag{33}$$

2.6. Current Effect

The current effect can be calculated by using Eq. 34-37, Where subscripts b and c represent the ship's body and current, respectively[35].

$$U = U_r = \sqrt{{u_r}^2 + {v_r}^2} \tag{34}$$

$$u = u_r = (u_b - u_c) = (u_b - U_c \cos \Psi_{c_r}) \tag{35}$$

$$v_m = v_r = (v_b - v_c) = (v_b - U_c \sin \Psi_{c_r}) \tag{36}$$

$$r = \Psi_{c_r}\ dan\ \Psi_{c_r} = \Psi - \Psi_c \tag{37}$$

3. Results and Discussion

The barge used in this research is BG. Winposh 3301 with the principal dimension shown in Table 5. The barge is simulated to berth at the multipurpose jetty of Paciran Port based on the trajectory obtained from AIS data. AIS is essential in this research because it can present ship traffic data and berthing-unberthing routes [36]. AIS provides a more comprehensive picture, but it contains too much irrelevant information. However, if used correctly, it can be helpful for many things [37]. Figure 2 shows the ship coming from the north with an initial speed of 0 knots, then heading south until berthing at the jetty of Paciran Port.

Table 5. Principal Dimension of BG. WINPOSH 3301

Main Principal	Dimension
LOA	100.58 m
LPP	96.56 m
Beam (B)	33.53 m
Height (H)	6.10 m
Draught (T)	4.71 m
Kecepatan (V)	5 Knot
Cb	0.88
Displacement	13,754.92 tons

Figure 2. Ships Berthing Trajectory at Paciran Port
Source: Marinetraffic.com

3.1. MATLAB Function

In Figure 3, for simulations using the Maneuvering Modeling Group (MMG) in MATLAB, it can start by creating the m-files F1, F2, and F3. The m-file F1 contains the forces acting on the ship along the x-axis, the m-file F2 contains the forces acting on the ship along the y-axis, and the m-file F3 contains the moment acting on the ship around the z-axis.

When creating the primary function, it is necessary to first define which variables are constant and which are variables. After that, make the 'for' loop logic from the beginning of the calculation to the end. The calculation starts with the values for current and wind. Then, it continues with the tugboat force, which uses 'if' logic.

Following that, there is a process of calling functions from m-file F1, m-file F2, and m-file F3. The output from these m-files is the acceleration along the x-axis, y-axis, and the angular acceleration around the z-axis. By calling the functions from these three m-files, the values of u, v, r, and heading at i+1 can be determined. The values of u, v, r, and heading at i+1 are then used in the looping calculation within the main file.

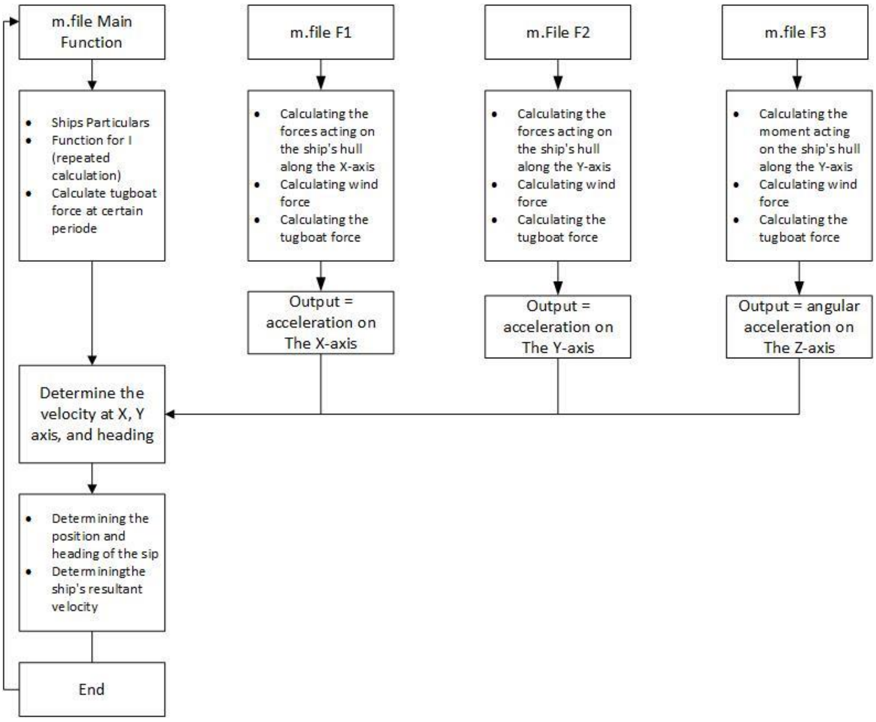

Figure 3. The Flowchart of MMG Simulation using MATLAB

3.2. Berthing Speed Acceptance Criteria and Environmental Condition

Table 5 shows that the displacement of the ship is 13,754.92 tons, to ensure the barge can berth safely. The barge's maximum berthing speed is 0.3 m/s during moderate conditions, as shown in Table 6. The more adverse the navigation conditions, from favourable to unfavourable, the higher the potential for an unexpected accident with the jetty [38].

Table 6. PIANC′ s Requirement of Berthing Speed for Ships

Vessel Displacement (tons)	Favourable Condition (m/s)	Moderate Condition (m/s)	Unfavourable Condition (m/s)
Under 10,000	0.2 – 0,16	0.45 – 0.3	0.6 – 0.4
10,000 – 50,000	0.12 – 0.08	0.3 – 0.15	0.45 – 0.22
50,000 – 100,000	0.08	0.15	0.2
Over 100,000	0.08	0.15	0.2

The simulations are conducted under normal environmental conditions and use two conditions. The current direction is from West to East for condition 1, and from East to West for condition 2. The parameters of environmental conditions are shown in Table 7. Environmental conditions are based on data from the Meteorology, Climatology, and Geophysics Agency.

Table 7. Environmental Condition Parameters

Environmental Condition	Condition 1	Condition 2
Wind Speed (Knots)	5	5
Wind Direction	Southeast to Northwest	Northwest to Southeast
Current Velocity (m/s)	0.44	0.31
Current Direction	West to East	East to West

3.3. MMG Simulation

According to the Minister of Transportation Regulation Number PM 57/ 2015, ships with a length of 70 m to 150 m must be assisted by at least one tugboat with a capacity of 2,000 horsepower and a minimum of 24 tons of bollard pull. This simulation assumes that a 30-ton bollard Pull tugboat pulls the barge. Uses four scenarios, each representing an environmental condition with two initial speed variations, 0 knots and 2.9 knots.

a. Scenario 1 (Condition 1 with initial speed 0 knots)

Figure 4 and Table 8 show barge speed, heading, trajectory, and tugboat procedure during the berthing process of scenario 1. The Barge has a speed of 0 knots at the initial condition with a heading of 210 degrees. The graph shows the ship′ s speed increasing from 0.8 knots to 2.2 knots at 900 seconds. This is an effect of the barge being pushed straight by the tug with 81% of its capacity. The influence of environmental conditions is immediately apparent at this stage. The current moves from west to east with a speed of 0.44 m/s, causing the barge to drift continuously to the east as it is towed forward. This drift is shown in the ship′ s trajectory in Figure 4-c, which curves slightly to the east. Therefore, the barge is braked with

85% power with a heading of 180 degrees until 1300 seconds, so the Barge′s speed becomes 0.8 knots, which not only serves to reduce speed but is also crucial for counteracting the current′s thrust. Furthermore, from 1300 to 1633 seconds, the Barge is turned by being pulled by a tugboat, so the barge′s heading becomes 300 degrees, parallel to the jetty. Finally, the ship will be moved to berth at the jetty with a speed of 0.278 knots or 0.143 m/s. The trajectory graph indicates that the barge remains within the Paciran Port channel, and the berth speed is still moderate according to the PIANC Standard.

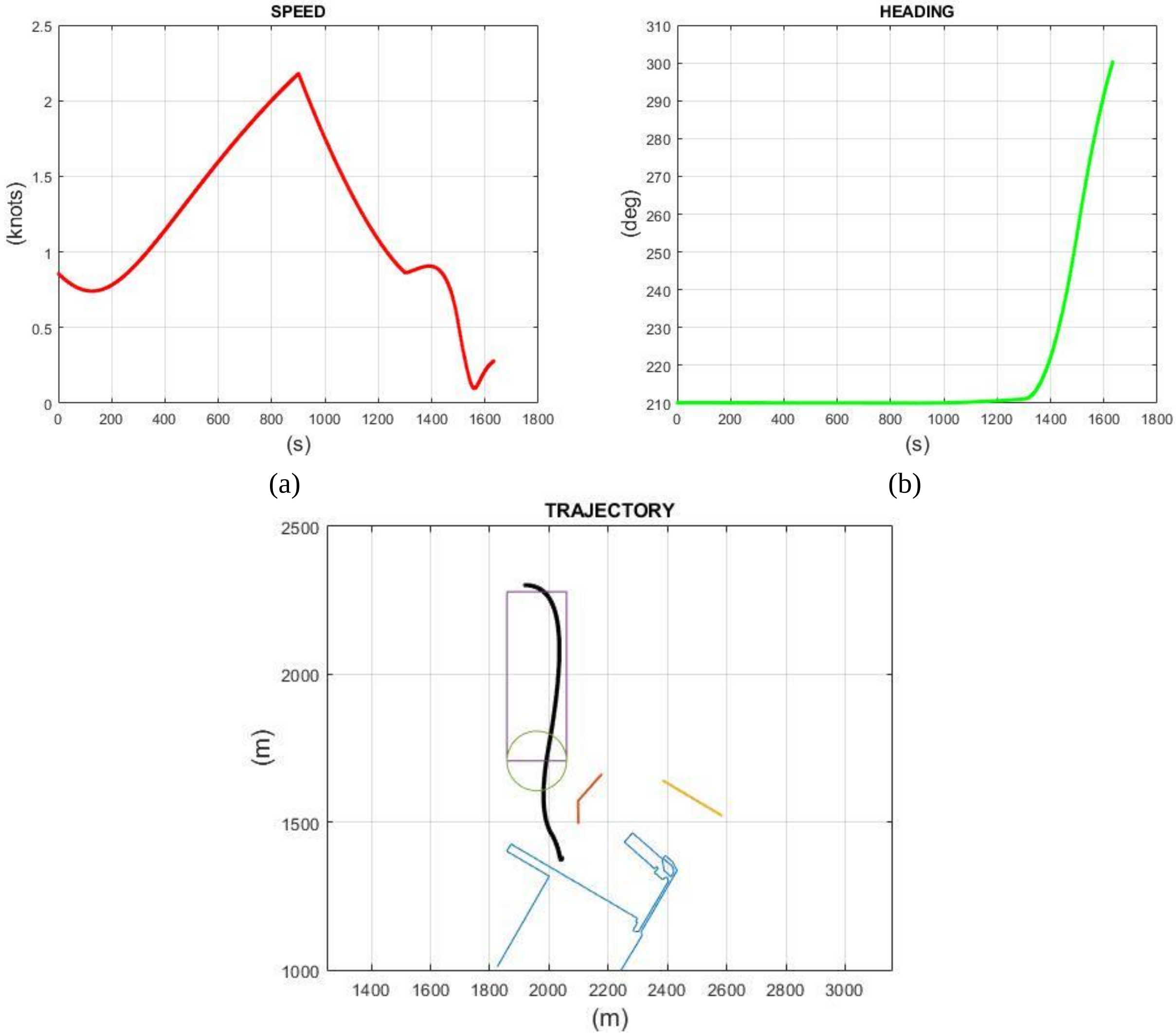

Figure 4. The Berthing Simulation Results of Scenario 1 (a) Speed, (b)Heading, and (c)Trajectory

Table 8. Tugboat Berthing Procedure of Scenario 1

Steps	Time (s)	Bollard Pull Percentage	Tugboat Direction
1	0 – 900	81%	0 degree
2	900 – 1300	85%	180 degrees
3	1300 – 1500	56%	22 degrees
4	1500 – 1633	35%	-25 degrees

b. Scenario 2 (Condition 1 with initial speed 2.9 knots)

Figure 5 and Table 9 show barge speed, heading, trajectory, and tugboat procedure during the berthing process of scenario 2. The Barge has an initial speed of 2.9 knots with a heading of 189 degrees, then pulls with 5% of the tugboat′s capacity and direction of -15 degrees. The barge's high initial speed of 2.9 knots significantly amplified the impact of the current moving from West to East. The combination of the significant forward momentum with the lateral force of the current resulted in an eastward drift, as seen in Figure 5-c. Consequently, a much more forceful response from the tugboat was required. Up to 95% of the brake force was essential to overcome the combined effects of the ship's inertia and the drift caused by the current. This maneuver successfully reduced the ship's speed to 1.3 knots with the barge′s heading of 175 degrees. Furthermore, between seconds 500 and 700, the barge is rotated so that its heading becomes 191 degrees. Then, between seconds 700 and 1000, braking is carried out with 95% power, resulting in a barge speed of 0.61 knots. The barge is rotated at seconds 1000 to 1172 so that the ship's heading becomes 300 degrees parallel to the jetty. In the end, the barge will be moved to the jetty at a speed of 0.219 knots or 0,112 m/s. The trajectory graph shows that the current carried the barge to the east, but it was still within the Paciran Port channel, and the berthing speed was still in a favourable condition according to the PIANC Standard.

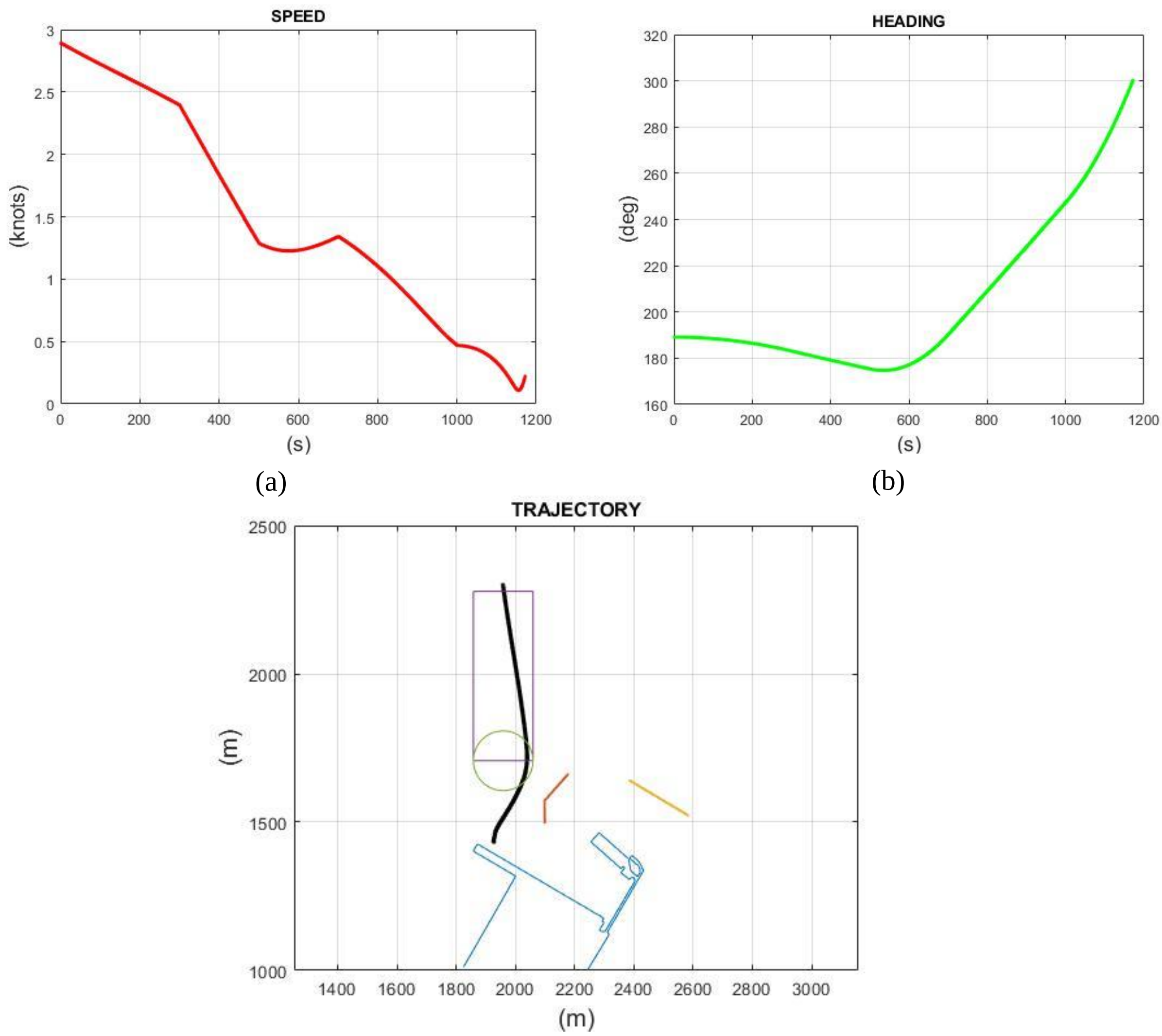

Figure 5. The Simulation Results of Scenario 2 (a) Speed, (b)Heading, and (c)Trajectory

Table 9. Tugboat Berthing Procedure of Scenario 2

Steps	Time (s)	Bollard Pull Percentage	Tugboat Direction
1	0 - 300	5%	-15 degree
2	300 – 500	95%	180 degrees
3	500 – 700	12%	115 degrees
4	700 – 1000	95%	180 degrees
5	1000 - 1172	31%	25 degrees

c. Scenario 3 (Condition 2 with initial speed 0 knots)

Figure 6 and Table 10 show barge speed, heading, trajectory, and tugboat procedure during the berthing process of scenario 3. The barge has an initial speed of 0 knots with a heading of 152 degrees. Then the barge moves straight, pulled by a tugboat with 65% power, for 850 seconds. The current comes from the west at a speed 0.31 m/s lower than in scenario 1 (0.44 m/s), causing the barge to drift to the west as seen in Figure 6 - c. However, the wind comes from the northwest and exerts a driving force from the southeast, partially counteracting the drift. This interaction between wind and current explains the relatively lower braking force required (39%) compared to scenario 1 (85%). The barge is braked with 39% power for 1300 seconds until the barge speed becomes 0.9 knots. Furthermore, from 1300 to 1852 seconds, the barge is rotated so that the barge's heading becomes 300 degrees. Then the barge will finally be berthed at the jetty at a speed of 0.398 knots or 0.2 m/s. The trajectory graph indicates that the barge is still inside the Paciran Port channel, and the berthing speed remains in moderate condition according to the PIANC Standard.

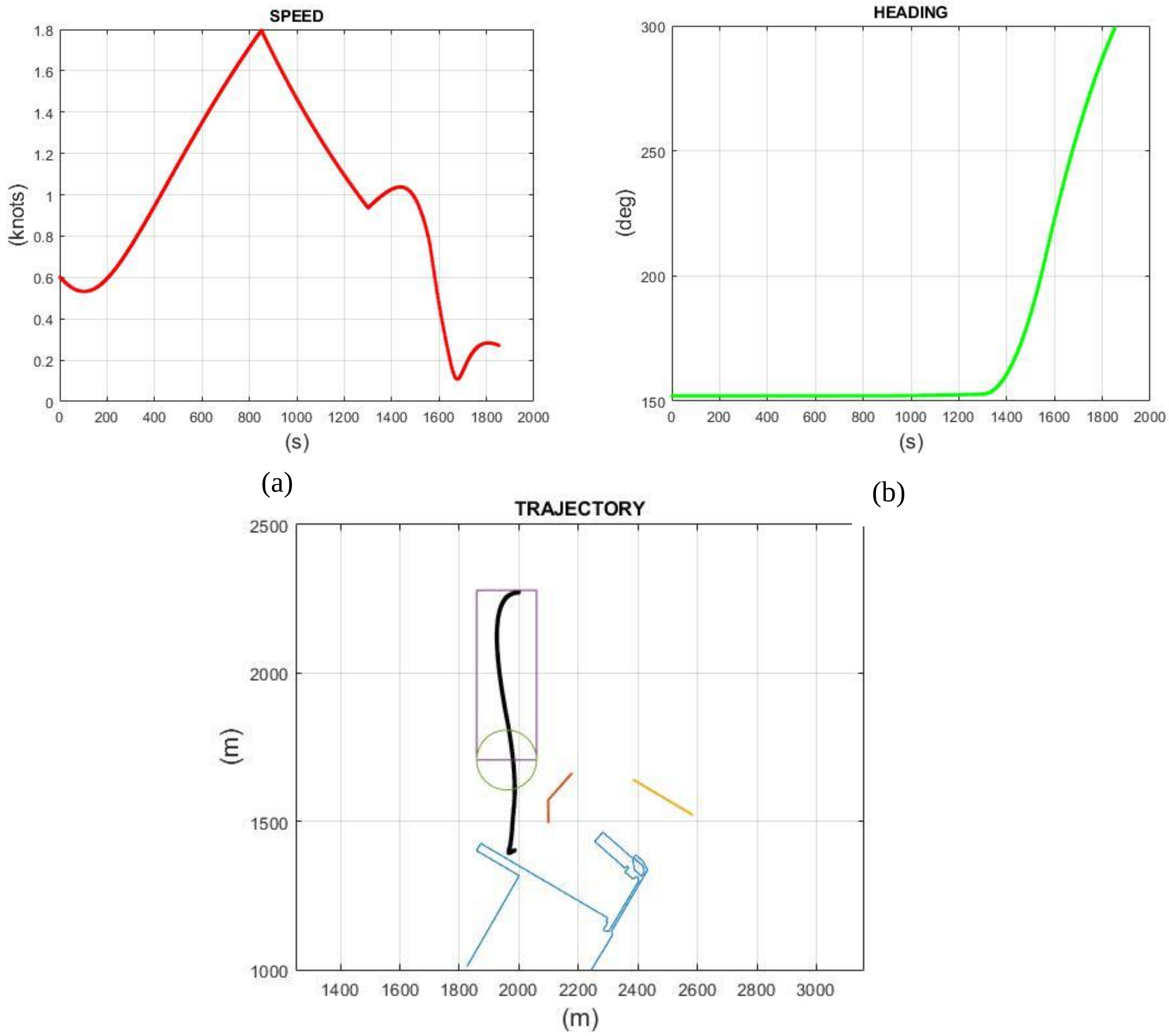

(c)

Figure 6. The Simulation Results of Scenario 3 (a) Speed, (b)Heading, and (c)Trajectory

Table 10. Tugboat Berthing Procedure of Scenario 3

Steps	Time (s)	Bollard Pull Percentage	Tugboat Direction
1	0 – 850	65%	0 degree
2	850 – 1300	39%	180 degrees
3	1300 – 1560	35%	26 degrees
4	1560 – 1852	35%	191 degrees

d. Scenario 4 (Condition 2 with initial speed 2.9 knots)

Figure 7 and Table 11 show barge speed, heading, trajectory, and tugboat procedure during the berthing process of scenario 4. The barge has an initial speed of 2.9 knots. Then the barge moves, pulled by a tugboat with 76% power, for 100 seconds. The simulation found the barge drifted to the east even though the current direction was towards the west. The ship's initial heading is 158 degrees, and the wind is blowing towards the Southeast with a speed of 5 knots. This means the wind is coming from the ship's portside (rear-left), and its direction is indeed almost parallel to the ship's forward direction. A wind from this direction will exert an aerodynamic force on the hull. Therefore, the wind itself contributes to a force component that pushes the ship to the east. Furthermore, the barge is braked with 50% power for 800 seconds until its speed reaches 0.8 knots. Furthermore, at the 800 to 1271 seconds, the barge is rotated so that the barge heading becomes 300 degrees parallel to the jetty. In the end, the barge will be berthed at the jetty with a speed of 0.132 knots or 0.067 m/s. The trajectory graph indicates that it is still within the Paciran Port channel, and the berthing speed remains in a favourable condition according to the PIANC Standard.

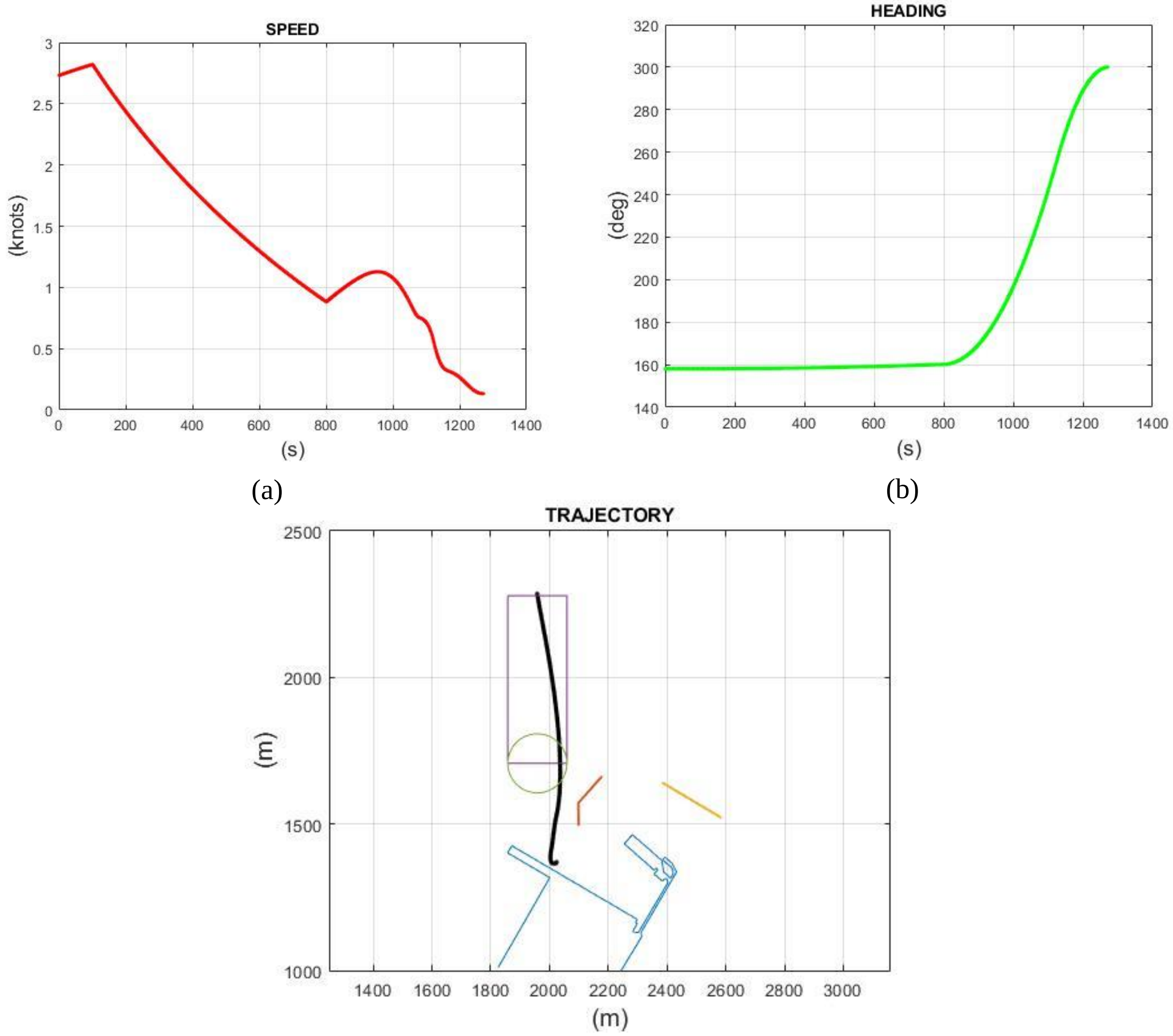

(c)
Figure 7. The Simulation Results of Scenario 4 (a) Speed, (b)Heading, and (c)Trajectory

Table 11. Tugboat Berthing Procedure of Scenario 4

Steps	Time (s)	Bollard Pull Percentage	Tugboat Direction
1	0 – 100	76%	0 degree
2	100 – 800	50%	180 degrees
3	800 – 1123	67%	15 degrees
4	1123 – 1271	65%	-35 degree

4. Conclusion

This research demonstrated the application of ship maneuvering simulations, utilizing the Maneuvering Modelling Group (MMG) model within MATLAB, to determine essential elements for safe tugboat handling during barge berthing operations at Paciran Port. By simulating various scenarios with differing environmental conditions and initial vessel speeds, this research provides a quantitative basis for understanding the interaction of forces and the required tugboat interventions to maintain control during the critical berthing phase. The results show that the element of tugboat handling (bollard pull percentage, direction, Time Series, and Duration) can assist the barge in safely navigating even with environmental disturbances, such as wind and current, with final berthing speeds consistently under 0.3 m/s, categorized as a moderate condition according to PIANC standards. The trajectory analyses further confirmed that the barge remained within the designated port channel during all simulated scenarios.

References

[1] G. Hejun, F. Fuquan, J. Xiaobin, W. Deling, and T. Qingfeng, "Ship Berthing Safety Assessment Based on Ship-Handling Simulator," *American Journal of Traffic and Transportation Engineering*, vol. 6, no. 1, p. 10, 2021, doi: https://doi.org/10.11648/j.ajtte.20210601.12.

[2] A. K. Vo, T. L. Mai, and H. K. Yoon, "Path Planning for Automatic Berthing Using Ship-Maneuvering Simulation-Based Deep Reinforcement Learning," *Applied Sciences*, vol. 13, no. 23, p. 12731, Nov. 2023, doi: https://doi.org/10.3390/app132312731.
[3] H.-T. Lee, J.-S. Lee, W.-J. Son, and I.-S. Cho, "Development of Machine Learning Strategy for Predicting the Risk Range of Ship's Berthing Velocity," *Journal of Marine Science and Engineering*, vol. 8, no. 5, p. 376, May 2020, doi: https://doi.org/10.3390/jmse8050376.
[4] V. Paulauskas, M. Simutis, B. Plačiene, R. Barzdžiukas, M. Jonkus, and D. Paulauskas, "The Influence of Port Tugs on Improving the Navigational Safety of the Port," *Journal of Marine Science and Engineering*, vol. 9, no. 3, p. 342, Mar. 2021, doi: https://doi.org/10.3390/jmse9030342.
[5] V. Paulauskas and D. Paulauskas, "Ship Mooring Methodology Designed for Ship Berthing in Extremely Limited Conditions," *Journal of Marine Science and Engineering*, vol. 13, no. 3, p. 575, Mar. 2025, doi: https://doi.org/10.3390/jmse13030575.
[6] G. Wu, X. Zhao, Y. Sun, and L. Wang, "Cooperative Maneuvering Mathematical Modeling for Multi-Tugs Towing a Ship in the Port Environment," *Journal of Marine Science and Engineering*, vol. 9, no. 4, p. 384, Apr. 2021, doi: https://doi.org/10.3390/jmse9040384.
[7] M. , & H. K. Sano, "A fundamental study on the ship handling simulation of tug–barge and pusher–barge systems for river service," ICSOT India: Coastal & Inland Shipping, 2015.
[8] Yangying. , C. Linying. , Z. Qingsong. , and S. Zhang. He, "Maneuvering Prediction of the Tugboat Vessel Based on CFD Methods," Paper presented at the The 33rd International Ocean and Polar Engineering Conference, 2023.
[9] T. Wu, R. Li, Q. Chen, G. Pi, S. Wan, and Q. Liu, "A Numerical Study on Modeling Ship Maneuvering Performance Using Twin Azimuth Thrusters," *Journal of Marine Science and Engineering*, vol. 11, no. 11, p. 2167, Nov. 2023, doi: https://doi.org/10.3390/jmse11112167.
[10] G. Taimuri, J. Matusiak, T. Mikkola, P. Kujala, and S. Hirdaris, "A 6-DoF maneuvering model for the rapid estimation of hydrodynamic actions in deep and shallow waters," *Ocean Engineering*, vol. 218, p. 108103, Dec. 2020, doi: https://doi.org/10.1016/j.oceaneng.2020.108103.
[11] B. Zhao, X. Zhang, and C. Liang, "A Novel Parameter Identification Algorithm for 3-DOF Ship Maneuvering Modelling Using Nonlinear Multi-Innovation," *Journal of Marine Science and Engineering*, vol. 10, no. 5, p. 581, Apr. 2022, doi: https://doi.org/10.3390/jmse10050581.
[12] Y. Xia, S. Zheng, Y. Yang, and Z. Qu, "Ship Maneuvering Performance Prediction Based on MMG Model," *IOP Conference Series: Materials Science and Engineering*, vol. 452, p. 042046, Dec. 2018, doi: https://doi.org/10.1088/1757-899X/452/4/042046.
[13] R. Okuda, H. Yasukawa, and A. Matsuda, "Validation of maneuvering simulations for a KCS at different forward speeds using the 4-DOF MMG method," *Ocean Engineering*, vol. 284, p. 115174, Sep. 2023, doi: https://doi.org/10.1016/j.oceaneng.2023.115174.
[14] K. Dai and Y. Li, "EXPERIMENTAL AND NUMERICAL INVESTIGATION ON MANEUVERING PERFORMANCE OF SMALL WATERPLANE AREA TWIN HULL," *Brodogradnja*, vol. 72, no. 2, pp. 93–114, Jun. 2021, doi: https://doi.org/10.21278/brod72206.
[15] A. Wicaksono, N. Hashimoto, and T. Takahashi, "Representation of small passenger ferry maneuvering motions by practical modular model," *International Journal of Naval Architecture and Ocean Engineering*, vol. 13, pp. 57–64, 2021, doi: https://doi.org/10.1016/j.ijnaoe.2020.12.006.
[16] Iswandi, R. Hidayat, and S. B. Wibowo, "An Evaluation Method of Ship-Tracking Algorithms for High-Frequency Surface Wave Radar considering High Maneuvers Generated by the MMG Model," *Journal of Engineering*, vol. 2023, pp. 1–13, May 2023, doi: https://doi.org/10.1155/2023/1481943.
[17] S. Zhang, Q. Wu, J. Liu, Y. He, and S. Li, "State-of-the-Art Review and Future Perspectives on Maneuvering Modeling for Automatic Ship Berthing," *Journal of Marine Science and Engineering*, vol. 11, no. 9, p. 1824, Sep. 2023, doi: https://doi.org/10.3390/jmse11091824.
[18] C. Chen, L. Zou, Z. Zou, and H. Guo, "Assessment of CFD-Based Ship Maneuvering Predictions Using Different Propeller Modeling Methods," *Journal of Marine Science and Engineering*, vol. 10, no. 8, p. 1131, Aug. 2022, doi: https://doi.org/10.3390/jmse10081131.
[19] A. H. Muhammad, . Syarifuddin, D. Paroka, S. Rahman, . Wisyono, and A. A. Pratama, "MANEUVERING PERFORMANCE OF A 30 GT FISHING VESSEL WITH ASYMMERICAL PROPELLER CONFIGURATION," *Jurnal Ilmu dan Teknologi Kelautan Tropis*, vol. 9, no. 2, pp. 491–498, Jan. 2018, doi: https://doi.org/10.29244/jitkt.v9i2.19314.
[20] I. Putu Sindhu Asmara and A. W. Husodo, "Ship to Ship Manoeuvring Simulation to Determine Elements of Tugboat Handling," *IOP Conference Series: Earth and Environmental Science*, vol. 1081, no. 1, p. 012014, Sep. 2022, doi: https://doi.org/10.1088/1755-1315/1081/1/012014.
[21] IPS. Asmara, E. Kobayashi, and T. Pitana, "Simulation of Collision Avoidance by Considering Potential Area of Water for Maneuvering based on MMG Model and AIS Data," in Proceedings of the 3rd International Conference on Simulation and Modeling Methodologies, Technologies and Applications, SciTePress - Science and and Technology Publications, 2013, pp. 243–250. doi: https://doi.org/10.5220/0004478002430250.

[22] A. Roubos, L. Groenewegen, and D. J. Peters, "Berthing velocity of large seagoing vessels in the port of Rotterdam," *Marine Structures*, vol. 51, pp. 202–219, Jan. 2017, doi: https://doi.org/10.1016/j.marstruc.2016.10.011.

[23] H. Yasukawa and Y. Yoshimura, "Introduction of MMG standard method for ship maneuvering predictions," *Journal of Marine Science and Engineering*, vol. 20, no. 1, pp. 37–52, Mar. 2015, doi: https://doi.org/10.1007/s00773-014-0293-y.

[24] V. V. Deogaonkar, A. K. Jadhav, K. Ramachandran, and A. S. Somayajula, "Data Driven Identification of Ship Maneuvering Coefficients," in Volume 5: Ocean Engineering, American Society of Mechanical Engineers, Jun. 2023. doi: https://doi.org/10.1115/OMAE2023-104644.

[25] S.-H. Kim, C.-K. Lee, and S.-M. Lee, "Estimation of Maneuverability of Fishing Vessel Considering Hull-Form Characteristics," *Journal of Marine Science and Engineering*, vol. 9, no. 6, p. 569, May 2021, doi: https://doi.org/10.3390/jmse9060569.

[26] O. F. Sukas, O. K. Kinaci, and S. Bal, "Theoretical background and application of MANSIM for ship maneuvering simulations," *Ocean Engineering*, vol. 192, p. 106239, Nov. 2019, doi: https://doi.org/10.1016/j.oceaneng.2019.106239.

[27] D. Clarke, P. Gedling, and G. T. Hine, "The Application of Manoeuvring Criteria in Hull Design Using Linear Theory," 1982. [Online]. Available: https://api.semanticscholar.org/CorpusID:199679024.

[28] Z. Zhou, S. Yan, and W. Feng, "Manoeuvring prediction of multiple-purpose cargo ships," *Ship Eng.*, vol. 6, pp. 21–36, 1983.

[29] Y. Yoshimura and Y. Masumoto, "Hydrodynamic Force Database with Medium High Speed Merchant Ships Including Fishing Vessels and Investigation into a Manoeuvring Prediction Method," *Journal of the Japan Society of Naval Architects and Ocean Engineers*, vol. 14, no., pp. 63–73, 2011, doi: https://doi.org/10.2534/jjasnaoe.14.63.

[30] H. Lee and S.-S. Shin, "The Prediction of ship's manoeuvring performance in initial design stage," 1998. [Online]. Available: https://api.semanticscholar.org/CorpusID:55072118

[31] K. , K. T. , N. Y. , & F. Y. Kijima, "On the manoeuvring performance of a ship with the parameter of loading condition," Autumn Meeting of the Society of Naval Architects of Japan, 1990.

[32] M. Maljković, I. Pavić, T. Meštrović, and M. Perkovič, "Ship Maneuvering in Shallow and Narrow Waters: Predictive Methods and Model Development Review," *Journal of Marine Science and Engineering*, vol. 12, no. 8, p. 1450, Aug. 2024, doi: https://doi.org/10.3390/jmse12081450.

[33] T. Fujiwara, M. Ueno, and T. Nimura, "Estimation of Wind Forces and Moments acting on Ships," *Journal of the Society of Naval Architects of Japan*, vol. 1998, no. 183, pp. 77–90, 1998, doi: https://doi.org/10.2534/jjasnaoe1968.1998.77.

[34] H. Yasukawa and R. Sakuno, "Application of the MMG method for the prediction of steady sailing condition and course stability of a ship under external disturbances," *Journal of Marine Science and Technology*, vol. 25, no. 1, pp. 196–220, Mar. 2020, doi: https://doi.org/10.1007/s00773-019-00641-4.

[35] I. Asmara and A. W. Husodo, "Ship to Ship Manoeuvring Simulation to Determine Elements of Tugboat Handling," *IOP Conference Series: Earth and Environmental Science*, vol. 1081, no. 1, p. 012014, Sep. 2022, doi: https://doi.org/10.1088/1755-1315/1081/1/012014.

[36] E. Lee, A. J. Mokashi, S. Y. Moon, and G. Kim, "The Maturity of Automatic Identification Systems (AIS) and Its Implications for Innovation," *Journal of Marine Science and Engineering*, vol. 7, no. 9, p. 287, Aug. 2019, doi: https://doi.org/10.3390/jmse7090287.

[37] T. Emmens, C. Amrit, A. Abdi, and M. Ghosh, "The promises and perils of Automatic Identification System data," *Expert Systems with Applications*, vol. 178, p. 114975, Sep. 2021, doi: https://doi.org/10.1016/j.eswa.2021.114975.

[38] A. A. Roubos, R. ; Williams, and P. Mirihagalla, "Recommendations for berthing velocity in PIANC WG211," in Proceedings of the 35th PIANC World Congres 2024, 2024, pp. 1050–1056.